

Famennian conodonts from the Esteghlal Refractories Mine, Abadeh area, south-central Iran

Mehdi Yazdi¹, Ali Meysami², Maryam Mannani³, Mohammad Hassan Bakhshaei¹ and Ruth Mawson⁴

¹Department of Geology, University of Isfahan, Iran;

²Department of Geology, University for Teacher Education, Tehran, Iran;

³Sepahan Refractory Mine Company, Isfahan, Iran;

⁴Macquarie University Centre for Ecostratigraphy and Palaeobiology, Macquarie University 2109, Australia.

Abstract – Various limestone bodies in the Esteghlal Refractories Mine in the Abadeh area of south-central Iran have produced conodonts consistent with the early Famennian Early or Middle *crepida* zones demonstrating that none of the limestone bodies are dramatically allochthonous with respect to one another. The age of volcanics associated with the early Famennian, Carboniferous and Permian units remains problematic; they are thought to be Late Permian age.

INTRODUCTION

The Esteghlal Refractories Mine (31°14'N, 52°28'E), 10 km northeast of Abadeh and 218 km SE of Isfahan (Figure 1), is the largest refractory clay mine in Iran with a total reserves of refractory minerals of around 85 million tons (Figures 2, 3.1). The deposit is located on the NE flank of a large anticlinal fold trending WNW; it has been dismembered into thrust blocks of various sizes by faulting believed to have been connected with the Central Iran and Zagros Thrust Zones. Typical of the Zagros Thrust structure is development of numerous subsidiary faults characterised, *inter alia*, by imbricate structures and thick crush zones. The main open cut mine is located in a block uplifted by movements associated with a substantial W- to NW-trending thrust (Figure 2); the latter has caused a Permian succession to have been thrust over Devonian formations. The area is seamed by sills and dikes of diabase and porphyrite 0.5 to 10 m in thickness (maximum 30 m). Rocks in the vicinity of the Esteghlal Refractories Mine are deeply weathered and to various degrees ferruginised (Figure 3.5, 3.6).

Attention focused on the area about the Esteghlal Refractory Mine during geological mapping of the Abadeh sheet in 1982 by a group of Iranian geologists led by one of us (Bakhshaei) with Russian associates (leader: Nicolai Padarai Gora). It was appreciated that the main carbonate-bearing intervals were almost certainly of Late Devonian age (Figure 3.2–4), but associated terrigenous deposits consisting of rhythmically alternating quartzose sandstones, quartzite and clastic limestones were thought to be Middle Devonian and perhaps Early Devonian in age. No

palaeontologic evidence has been forthcoming to support this view, based solely on stratigraphic position.

Three principal Devonian units can be discriminated in the area about the Esteghlal Refractory Mine: a lower interval of calcareous arenaceous rocks, a middle interval of rather similar lithologies, and an upper interval of sandy shale. Lithologic changes occur from bed to bed reflecting variation in the nature of sedimentation and the

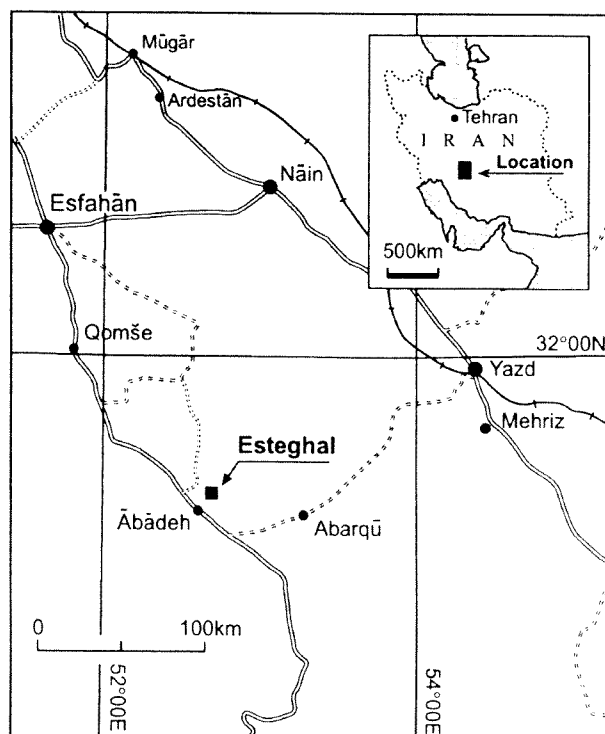


Figure 1 Location of the Esteghlal Refractories Mine in south central Iran.

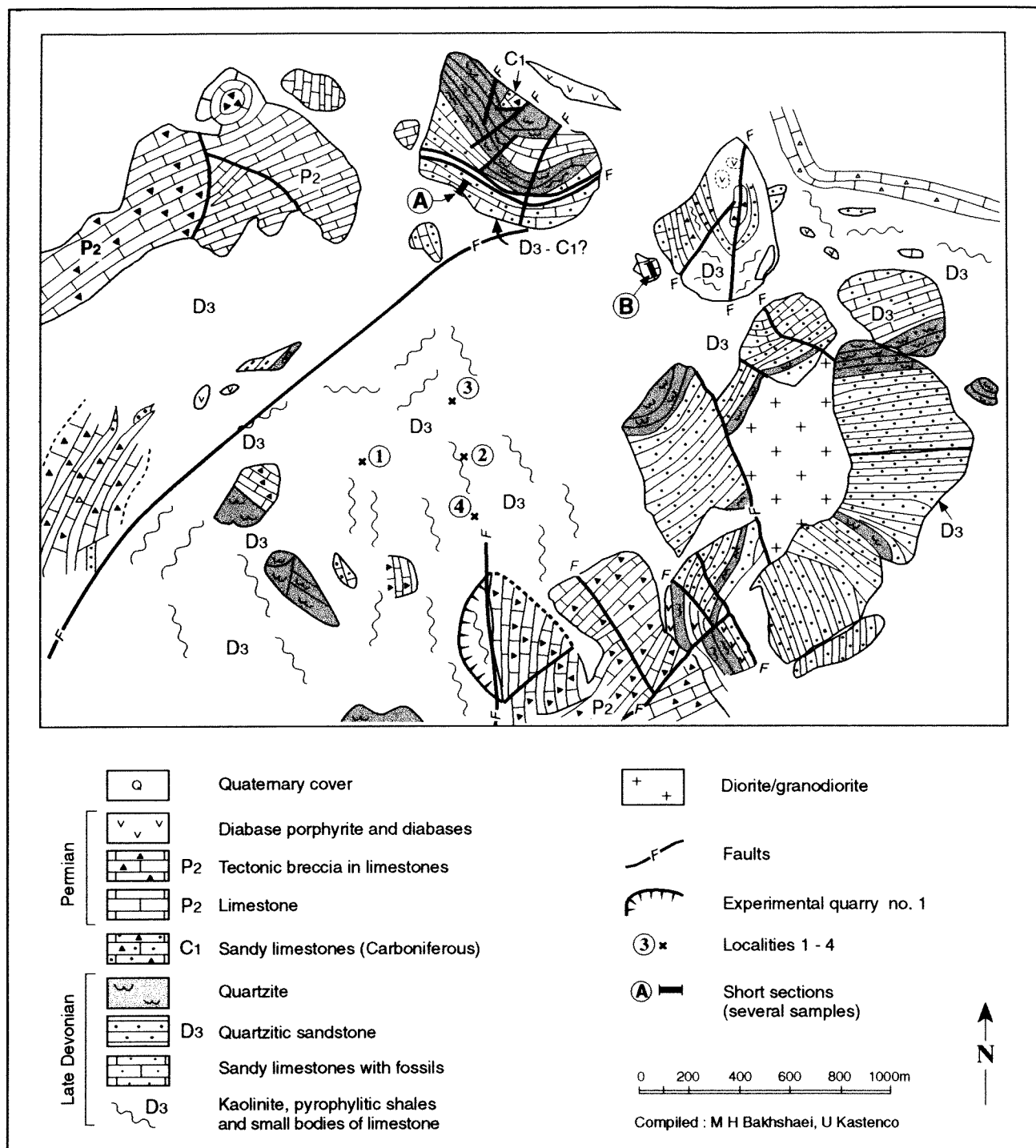
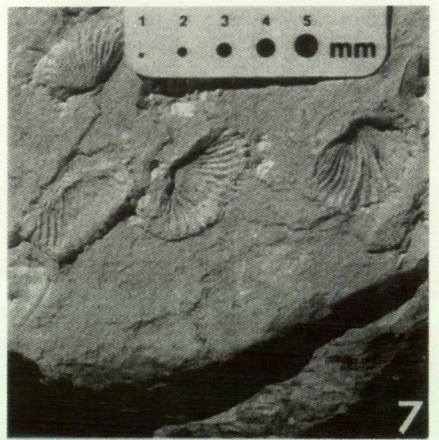


Figure 2 Geology of the study area showing location of Sections A and B and spot localities 1-4 from which conodonts were recovered.

extensive post-depositional kaolinitization, apparently during Late Devonian times. The pyrophyllitic shales, the focus of extraction of refractory raw materials, are restricted to the upper unit of sandy shales. They occur with intervals of sandy rocks (sandstones and limestones) from 10-20 cm in thickness up to 5-10 m in thickness. Macrofossils from this unit—brachiopods, gastropods, bivalves crinoid stems and rare ammonoids (especially locality 1, Figures 2, 3.7, 8)—

have been changed post-mortally into aluminosilicates: pyrophyllite, diaspore, illite, kaolinite and rare boehmite, leaving virtually no trace of phosphate or calcium carbonate.

About 10 years ago, one of us (Bakhshaei) noted the presence of a Late Devonian fauna including species of brachiopods – *Aulacella*, *Cyrtiopsis*, *Cleiothyridina*, *Cyrtospirifer* – and rare trilobites indicative of a broad Famennian age, but important problems remained, above all to determine if rocks



Remarks

I. a. alternatus has been reported to occur in Early and Middle *crepida* zones in many parts of the world, for example in western Pomerania (Matyja 1993), in western USA and Belgium (Sandberg and Dreesen 1984), South China (Ji and Ziegler 1993) and Iran (Yazdi 1999).

***Icriodus alternatus mawsonae* Yazdi, 1999**

Figure 4.9–13

Icriodus alternatus n. subsp.: Clausen, Korn and Luppold 1991: pl. 8, fig. 4.

Icriodus alternatus mawsonae: Yazdi 1999: 197, pl. 1, fig. 15, pl. 2, figs 3, 4.

Icriodus alternatus mawsonae: Talent *et al.* 1999: pl. 5, fig. 9.

Remarks

Specimens recovered from the Esteghlal Refractories Mine assigned to *Icriodus alternatus mawsonae* are very close to those from eastern Iran illustrated by Yazdi (1999). According to Yazdi, (1999) the age-range of this subspecies is from Late *triangularis* Zone to Early *crepida* Zone. Faunas consistent with this age from northeast Pakistan that include *I. a. mawsonae* have recently been documented by Talent *et al.* (1999).

***Icriodus homeomorphus* Mawson, 1999**

Figure 4.2–4

Icriodus homeomorphus Mawson: Talent *et al.* 1999: 216–217, pl. 5, figs 2–5, 8, 12–14, pl. 7, figs 13, 14, 16.

Icriodus alternatus morphotype 2: Yazdi 1999: pl. 1, figs 11, 13, 14.

Remarks

First described from the Shogram Formation, Kuragh Spur, northwest Pakistan (Talent *et al.* 1999), *I. homeomorphus* closely resembles icriodontids commonly found in the Middle Devonian. Yazdi's (1999, Pl. 1, figs 11, 13, 14) illustrations of *I. alternatus* morphotype 2 from his Howz-e-Dorah section in eastern Iran, have been referred to the new species which is broader in

outline than *I. alternatus*. In both Pakistan and Iran *I. homeomorphus* occurs in faunas argued to have an age range from Late *triangularis* Zone to Early *crepida* Zone.

***Icriodus iowaensis iowaensis* Youngquist and Peterson, 1947**

Figure 4.1

Icriodus iowaensis iowaensis Youngquist and Peterson 1947: 247, pl. 37, figs 22–24, 27–29.

Icriodus iowaensis iowaensis: Johnston and Chatterton 1991: pl. 3, figs 21–24.

Icriodus iowaensis iowaensis: Bender and Piecha 1991: Table 1, figs 3–4.

Icriodus iowaensis: Hladil *et al.* 1991: pl. 15, fig. 5.

Icriodus iowaensis iowaensis: Savage 1992: 280, figs 2.1–2.6.

Icriodus iowaensis iowaensis: Ji and Ziegler 1993: 56, Text-fig. 6 fig. 8.

Icriodus iowaensis iowaensis: Yazdi 1999: pl. 1, figs 1–9.

Remarks

According to Sandberg and Dreesen (1984), the age-range of this subspecies is from Middle *triangularis* Zone into Early *rhomboidea* Zone.

Genus *Pelekysgnathus* Thomas, 1949**Type species***Pelekysgnathus inclinatus* Thomas, 1949***Pelekysgnathus inclinatus* Thomas, 1949**

Figure 4.15–18

Pelekysgnathus inclinatus Thomas 1949: 424–425, pl. 2, fig. 10.

Pelekysgnathus inclinatus: Sandberg and Dreesen 1984: 161, pl. 3, figs 5, 7–9: P1.4, figs 7–9.

Pelekysgnathus inclinatus: Metzger 1989: 516, fig. 13, 23, 25.

Pelekysgnathus inclinatus: Molloy *et al.* 1997: 10, pl. 4, figs 4–7.

Figure 3 Limestones and nodules cropping out in the quarry area. 1, General view of the Estaghal Refractories Mine. Note the stockpile of mined refractory clays in the foreground ready for transport. 2, Limestone block, source of Sample 2, standing out from the more weathered refractory clays. 3, Limestone horizon, source of Sample 1, showing bedding parallel with the refractory clays. 4, Close-up of limestone horizon from which Sample 4 was derived. 5, Nodules and concentration of refractory clays mixed with hematite. 6, Enlargement of broken nodule shown above. Note concentric banding. 7, Spiriferid brachiopods with calcareous shells altered to refractory minerals. 8, Tiny, deformed crinoid ossicles altered to refractory minerals and replaced by calcite, hematite and aluminosilicates.

Pelekysgnathus inclinatus: Yazdi 1999: pl. 2, figs 16–17.

Remarks

Cone elements recovered from the Esteghlal Refractories Mine were assigned to *Pelekysgnathus inclinatus* on the basis of size and position of the basal cavity. According to Sandberg and Dreesen (1984) the age-range of this subspecies is from the base of the Early *crepida* Zone into Late *praesulcata* Zone.

Genus *Polygnathus* Hinde, 1879

Type species

Polygnathus dubius Hinde, 1879

Polygnathus buzmakovi Kuz'min, 1991

Figure 5.14, 15

Polygnathus buzmakovi Kuz'min 1991: 70, pl. 4, figs 1–5.

Polygnathus buzmakovi: Molloy *et al.* 1997: pl. 6, figs 3–5.

Remarks

According to Kuz'min (1990), *P. buzmakovi* is restricted to the *crepida* Zone. As yet it has been reported only from localities along the northern margin of Gondwana.

Polygnathus brevilaminus Branson and Mehl, 1934

Figure 5.9–11

Polygnathus brevilaminus Branson and Mehl 1934: 246, pl. 21, figs 3–6.

Polygnathus brevilaminus: Klapper and Lane 1985: 934.

Polygnathus brevilaminus: Metzger 1989: 518, Figure 15.4.

Remarks

This species appears to be a relatively long-ranging species: Barskov *et al.* (1991) suggest a range from *gigas* Zone to *marginifera* Zone, Ji and Ziegler (1993) suggest it may have originated in the Frasnian.

Polygnathus communis communis

Branson and Mehl, 1934

Figure 5.17

Polygnathus communis communis Branson and Mehl 1934: 293, pl. 24, figs 1–4.

Polygnathus communis communis: Gagiev and Kononova 1990: pl. 3, figs 13, 22, pl. 4, figs 20, 21.

Polygnathus communis communis: Johnston and Chatterton 1991: 171, pl. 2, figs 11–12.

Polygnathus communis communis: Bender, Braun and Königshof 1991: pl. 2, fig. 1.

Polygnathus communis communis: Ji and Ziegler 1993: 76, pl. 35, figs 4–6.

Polygnathus communis communis: Wang 1993: 231, pl. 40, fig. 13, pl. 41, figs 11a,b, 12a,b.

Polygnathus communis communis: Pickett 1994: 54, fig. 2.2.

Polygnathus communis communis: Molloy *et al.* 1997: 12, pl. 8, figs 4,5.

Polygnathus communis communis: Yazdi 1999: pl. 7, figs 13,15.

Remarks

Two polygnathid specimens recovered from the Esteghlal Refractories Mine are assigned to *Polygnathus communis communis* on the basis of shagreen platform and configuration of the basal features. While Ji and Ziegler (1993: 76) consider this subspecies to first appear Middle *crepida* Zone, Barskov *et al.* (1991) show it to be present in the Early *crepida* Zone.

Polygnathus pennatulus Ulrich and Bassler, 1926

Figure 5.8

Polygnathus pennatulus Ulrich and Bassler 1926: 45, pl. 7, fig. 8.

Polygnathus pennatulus: Metzger 1989: 520, Figure 15.12–15, 23.

Remarks

This species has been reported to occur in faunas consistent with the Early *crepida* Zone or younger (Metzger 1989).

Polygnathus cf. politus Ovnatanova, 1969

Figure 5.18

Polygnathus politus Ovnatanova 1969: 140, figs 4, 5.

Polygnathus pacificus: Savage and Funai 1980: 811, pl. 2, figs 6–17.

Polygnathus politus: Talent *et al.* 1999: pl. 7, figs 11a, b.

Remarks

The single polygnathid from Section A, sample 6 has been identified as *P. cf. politus*. In the Kuragh

Spur section in northernmost Pakistan (Talent *et al.* 1999), similar forms have been dated as Late *triangularis* to Early *crepida* Zone. Although *P. politus* has been recovered from horizons as old as *gigas* Zone (Ovnatanova 1969), Section A, sample 16 has yielded *P. communis communis* indicating a younger age in the present instance.

***Polygnathus procerus* Sannemann, 1955**

Figure 5.12, 13

Polygnathus procerus Sannemann 1955: 55, pl. 1, fig. 11.

Polygnathus procerus: Matyja and Zbikowska 1974: 782, pl. 6, figs 3, 4.

Polygnathus procerus: Wang and Ziegler 1983: pl. 7, figs 12a, 12b.

Polygnathus procerus: Ji and Ziegler 1993: 83–84, pl. 38, figs 4–8, test-fig. 21, fig. 1).

Remarks

Two polygnathid specimens recovered from Samples 1 and 3 are referred to *P. procerus* on the basis of their arched, lanceolate platforms and extended carinas. Ji and Ziegler (1993) report this species from horizons in South China from within the Middle *falsiovalis* Zone through into the Late *crepida* Zone.

***Polygnathus semicostatus* Branson and Mehl, 1934**

Figure 5.16

Polygnathus semicostatus Branson and Mehl 1934: 247–248, pl. 21, figs 1, 2.

Polygnathus semicostatus: Dreesen, Orchard and Bouckaert 1974: 17, pl. 1, fig. 7.

Polygnathus semicostatus: Sandberg and Ziegler 1979: 187, pl. 5, figs 1–5.

Polygnathus semicostatus: Wang and Ziegler 1982: 155, pl. 1, figs 23, 30, 31.

Polygnathus semicostatus: Metzger 1989: 521, Fig. 15 N. 17.

Polygnathus semicostatus: Johnston and Chatterton 1991: pl. 2, fig. 8.

Polygnathus semicostatus: Ji and Ziegler 1993: 84, Text-fig. 19, fig. 4.

Polygnathus semicostatus: Molloy *et al.* 1997: 12, pl. 5, figs 3, 7, pl. 4, fig. 14.

Remarks

Polygnathus semicostatus has not been recovered from horizons older than Middle *crepida* Zone, for example, in Belgium (Dreesen and Duser 1974), in

south China (Ji and Ziegler 1993) and Iran (Yazdi 1999). Its occurrence in Sample 3 in the Estaghlal Mine suggests that this horizon is slightly younger than the other limestone horizons.

Order Ozarkodinida Dzik, 1976

Family Palmatolepidae Sweet, 1988

Genus *Palmatolepis* Ulrich and Bassler, 1926

Type species

Palmatolepis perlobata Ulrich and Bassler, 1926

***Palmatolepis quadrantinosalobata* Sannemann, 1955**

Figure 5.6, 7

Palmatolepis quadrantinosalobata Sannemann 1955: 328, pl. 24, fig. 6.

Palmatolepis quadrantinosalobata: Ji 1989: pl. 2, figs 23–24.

Palmatolepis quadrantinosalobata: Johnston and Chatterton 1991: pl. 1, figs 14–16.

Palmatolepis quadrantinosalobata: Belka *et al.* 1992: pl. 3, figs 4.

Palmatolepis quadrantinosalobata: Savoy and Harris 1993: 2410, fig. 29.

Palmatolepis quadrantinosalobata: Ji and Ziegler 1993: 69, pl. 23, figs 5–7.

Remarks

Palmatolepis quadrantinosalobata has been documented by Ji and Ziegler (1993: 69), from horizons in South China ranging in age from the Early *crepida* Zone into the Early *rhomboidae* Zone (Famennian). This is in accord with the age-range given by Ziegler (1973).

Palmatolepis subperlobata

Branson and Mehl, 1934

Figure 5.1

Palmatolepis subperlobata Branson and Mehl 1934: 235, pl. 18, figs 11, 21.

Palmatolepis subperlobata: Ji 1989: pl. 2, figs. 25–27.

Palmatolepis subperlobata: Johnston and Chatterton 1991: pl. 1, figs 20, 24.

Palmatolepis subperlobata: Ji and Ziegler 1993: 72, pl. 20, figs 3–9. pl. 21, figs 11–12, text-fig. 16, figs 5, 6, 8.

Palmatolepis subperlobata: Metzger 1994: 638–639, figs 17.2, 3, 7, 10.

Palmatolepis subperlobata: Over 1997: 170–171, Figure 10.2, 3, 6, 7, 9.

Palmatolepis subperlobata: Yazdi 1999: pl. 10, figs 6, 7, 14.

Remarks

A single palmatolepid specimen from Sample 1 is referred to *Pal. subperlobata* rather than *Pal. triangularis* because of its shagreen surface ornament compared to the nodose surface of the latter. Although the specimen occurs in a fauna that includes *Pal. tenuipunctata*, its platform is insufficiently narrow to be referred to that species. According to Ji and Ziegler (1993: 72), *Pal. subperlobata* is found in South China in horizons of Middle *triangularis* into Early *marginifera* Zone. Over (1997) states the species first occurs in Early *triangularis* Zone.

Palmatolepis tenuipunctata Sannemann, 1955 Figures 5.2–4

Palmatolepis tenuipunctata Sannemann 1955: 136, pl. 6, fig. 22.

Palmatolepis tenuipunctata: Ji 1989: pl. 2, fig. 14.

Palmatolepis tenuipunctata Johnston and Chatterton 1991: 169, pl. 1, fig. 18.

Palmatolepis tenuipunctata: Ji and Ziegler 1993: 639, fig. 17, 22.

Palmatolepis tenuipunctata: Metzger 1994: 639, fig. 17, 22.

Palmatolepis tenuipunctata: Phuong and Weyant 1994: 133, pl. 1, figs 9, 10.

Remarks

According to Ji and Ziegler (1993), this subspecies has an age-range from Late *triangularis* Zone to the latest *crepida* Zone in sections in South China; elsewhere it has been identified in horizons of Early *triangularis* Zone (e.g. Ziegler 1973).

ACKNOWLEDGEMENTS

Support for field expenses was provided by the geology departments of the University of Isfahan and the University of Teacher Education, Tehran. SEM photos were provided by the Macquarie University Centre for Ecostratigraphy and Palaeobiology. We thank colleagues in our respective institutions for providing encouragement to extract information from the structurally complicated mine area. Constructive comment on the paper by two assessors is gratefully acknowledged. This is a contribution to IGCP Project 421 *North Gondwana mid-Palaeozoic bioevent/biogeography patterns in relation to crustal dynamics*.

REFERENCES

- Barskov, I.S., Vorsontsova, T.N., Kononova, L.I. and Kuz'min, A.V. (1991). Index conodonts of the Devonian and Early Carboniferous: 1–183, Moscow University, Moscow.
- Belka, Z., Groessen, E. and Wendt, J. (1992). Conodont biofacies patterns in the Kellwasser Facies (Upper Frasnian/Lower Famennian) of the eastern Anti Atlas, Morocco. *Palaeogeography, Palaeoclimatology, Palaeoecology* 91:143–173.
- Bender, K.P. and Piecha, P. (1991). Ein neues Vorkommen Von Unterem und Oberem Kellwasser- Horizont in der Beckenfazies der Dill- Mulde (Oberdevon, Rheinisches Schiefergebirge). *Geologica et Palaeontologica* 25: 37–45.
- Bender, K.P., Braun, A. and Königshof, P. (1991). Radiolarian und conodonten aus unterkarbonischen Kieselkalken und Kieselschiefern des nordlichen Sechiefergebirges. *Geologica et Palaeontologica* 25: 87–97.
- Branson, E.B. and Mehl, M.G. (1934). Conodonts from the Grassy Creek Shale of Missouri. *University of Missouri Studies* 8:171–259.
- Clausen, C.D., Korn, D. and Luppold, F.W. (1991). Litho- und Biofazies des middle- bis oberdevonischen karbonatprofiles am Beringhauaer Tunnie Messinghauser Sattel, Nordliches Rheinisches Schiefergebirge). *Geologie und Paläontologie, Westfalen* 18: 7–16.
- Dreesen, R. and Duser, M. (1974). Refinement of conodont-biozonation in the Famenne-type area. *Service géologique de Belgique Publication* 13: 1–36.
- Dreesen, R., Orchard, M.J. and Bouckaert, J. (1974). Intraspecific morphological variation within the *Polygnathus semicostatus* Branson Mehl. *Service géologique de Belgique Publication* 22: 1–8.
- Gagiev, M.H. and Kononova, L.I. (1990). The Upper Devonian and Lower Carboniferous sequences in the Kamenka River section (Kolyma River Basin, the Soviet North-East) stratigraphic description. Conodonta. *Courier Forschungsinstitut Senckenberg* 118: 81–103.
- Hhadil, J., Krejci, Z., Kalvoda, J., Ginter, M., Galle, A. and Berousek, P. (1991). Carbonate ramp environment of the Kellwasser time-interval (Lesnilom, Moravia, Czechoslovakia). *Bulletin de la Société de Belge de Géologie* 100: 57–119.
- Ji, Q. (1989). On the Frasnian–Famennian mass extinction event in South China. *Courier Forschungsinstitut Senckenberg* 117: 275–301.
- Ji, Q. and Ziegler, W. (1993). The Lali section: An excellent Reference section for Upper Devonian in south China. *Courier Forschungsinstitut Senckenberg* 157: 1–183.
- Johnston, D.I. and Chatterton, B.D.E. (1991). Famennian conodont biostratigraphy of the Palliser Formation, Rocky Mountains, Alberta and British Columbia. In Orchard, M.J. and McCracken, A.D. (eds), Ordovician to Triassic conodont paleontology of the Canadian Cordillera. *Geological Survey of Canada Bulletin* 417: 163–183.
- Klapper, G. and Lane, H.R. (1985). Upper Devonian

- (Frasian) conodonts of the *Polygnathus* biofacies, N.W.T., Canada. *Journal of Paleontology* **59**: 904–951.
- Kuz'min, A. (1991). Asymmetrical paired platform elements and some specimens of the genus *Polygnathus* [conodonts]. *Paleontological Journal* **1991**(4): 62–70. [translated from Russian]
- Matyja, H. (1993). Upper Devonian of Western Pomerania. *Acta Geologica Polonica* **43**: 27–94.
- Matyja, H. and Zbikowska, B. (1974). Stratigrafia dewonu górnego profilu wiercenia Minkowice 1 (basen lubelski). (Stratigraphy of the Upper Devonian from the borehole Minkowice 1 [Lublin Basin]). *Acta Geologica Polonica* **24**: 663–694.
- Metzger, R. (1989). Upper Devonian (Frasnian–Famennian) conodont biostratigraphy in the subsurface of north-central Iowa and southeastern Nebraska. *Journal of Paleontology* **63**: 503–524.
- Metzger, R. (1994). Multielement reconstruction of *Palmatolepis* and *Polygnathus* (Upper Devonian, Famennian) from the Canning Basin, Australia and Bactrian Mountains, Nevada. *Journal of Paleontology* **68**: 617–647.
- Molloy, P.D., Talent, J.A. and Mawson, R. (1997). Late Devonian–Tournaisian conodonts from the eastern Khyber Region, north-west Pakistan. *Rivista Italiana di Paleontologia e Stratigrafia* **103**: 123–148.
- Phuong, T.H. and Weyant, M. (1994). Discovery of Famennian conodonts from the Quyet Thang Mountain, north of the town of Thanh Hoa, Vietnam. *Courier Forschungsinstitut Senckenberg* **168**: 131–137.
- Over, D.J. (1997). Conodont biostratigraphy of the Java Formation (Upper Devonian) and the Frasnian–Famennian boundary in western New York State. *Geological Society of America Special Paper* **321**: 161–177.
- Ovnatanova, N.S. (1969). Nevye verknedevoevskie konodonty tsentral'nykh rayonov Russkoy Platformy i Timana. (New Upper Devonian conodonts from central regions of the Russian Platform and the Timan.) *Vsesoyuznyy Nauchno-Issledovatel'skiy Geologorazvedochnyy Neftyanoy Institut, Trudy, Vypusk* **93**: 139–141.
- Pickett, J.W. (1994). Tournaisian corals and conodonts from the Slaughterhouse Creek area, New South Wales, Australia. *Courier Forschungsinstitut Senckenberg* **172**: 51–67.
- Sandberg, C.A., and Dreesen, R. (1984). Late Devonian icriodontid biofacies models and alternate shallow-water conodont zonation. *Geological Society of America Special Paper* **196**: 143–178.
- Sandberg, C.A. and Ziegler, W. (1979). Taxonomy and biofacies of important conodonts of Late Devonian *styriacus*-Zone, United States and Germany. *Geologica et Palaeontologica* **13**: 173–212.
- Sannemann, D. (1955). Beitrag zur Unterliederung des Oberdevons nach Conodonten. *Neues Jahrbuch für Geologie und Paläontologie, Abhandlungen* **100**: 324–331.
- Savage, N.M. (1992). Late Devonian (Frasnian and Famennian) conodonts from the Wadleigh limestone, southeastern Alaska. *Journal of Paleontology* **66**(2): 277–292.
- Savage, N.M. and Funai, C.A. (1980). Devonian conodonts of probably early Frasnian age from the Coronados Islands of southeastern Alaska. *Journal of Paleontology* **54**: 806–813.
- Savoy, L.E. and Harris, A.G. (1993). Conodont biofacies and taphonomy along a carbonate ramp to black shale basin (latest Devonian and earliest Carboniferous), southernmost Canadian Cordillera and adjacent Montana. *Canadian Journal of Earth Science* **30**: 2404–2422.
- Sweet, W.C. (1988). The Conodonta: Morphology, taxonomy, paleoecology, and evolutionary history of a long-extinct animal phylum. *Monographs on Geology and Geophysics* **10**: 1–291, Clarendon Press, Oxford.
- Talent, J.A., Gaetani, M., Mawson, R., Molloy, P.D. and Conaghan, P.J. [with a contribution from Lehnert, O. and Trotter, J.A.] (1999). Early Ordovician and Devonian conodonts from the Western Karakoram and Hindu Kush, northernmost Pakistan. *Rivista Italiana di Paleontologia e Stratigrafia* **105**: 201–230.
- Thomas, L. A. (1949). Devonian–Mississippian formations of southeast Iowa. *Geological Society of America Bulletin* **60**: 403–438.
- Ulrich, E.O. and Bassler, R.S. (1926). A classification of the toothlike fossils, conodonts, with description of American Devonian and Mississippian species. *Proceedings of the United States National Museum* **68**: 1–63.
- Wang, C.Y. (1993). Conodonts of Lower Yangtze Valley and index to biostratigraphy and organic metamorphic maturity: 1–326. Sciences Publishing House, Beijing.
- Wang, C.Y. and Ziegler, W. (1982). On the Devonian–Carboniferous boundary in south China based on conodonts. *Geologica et Palaeontologica* **16**: 151–162.
- Wang, C.Y. and Ziegler, W. (1983). Devonian Conodont biostratigraphy of Guangxi, south China, and the correlation with Europe. *Geologica et Palaeontologica* **17**: 183–220.
- Youngquist, W.L. and Peterson, R.F. (1947). Conodonts from the Sheffield Formation of North-central Iowa. *Journal of Paleontology* **21**: 242–253.
- Yazdi, M. (1999). Late Devonian–Carboniferous conodonts from eastern Iran. *Rivista Italiana di Paleontologia e Stratigrafia* **105**: 167–200.
- Ziegler, W. (ed). (1973). Catalogue of conodonts, Volume I: 1–504, 27 pls, E. Schweizerbart'sche Verlagsbuchhandlung, Stuttgart.
- Ziegler, W. and Sandberg, C.A. (1984). *Palmatolepis*-based revision of upper part of standard late Devonian conodont zonation. *Geological Society of America Special Paper* **196**: 179–194.

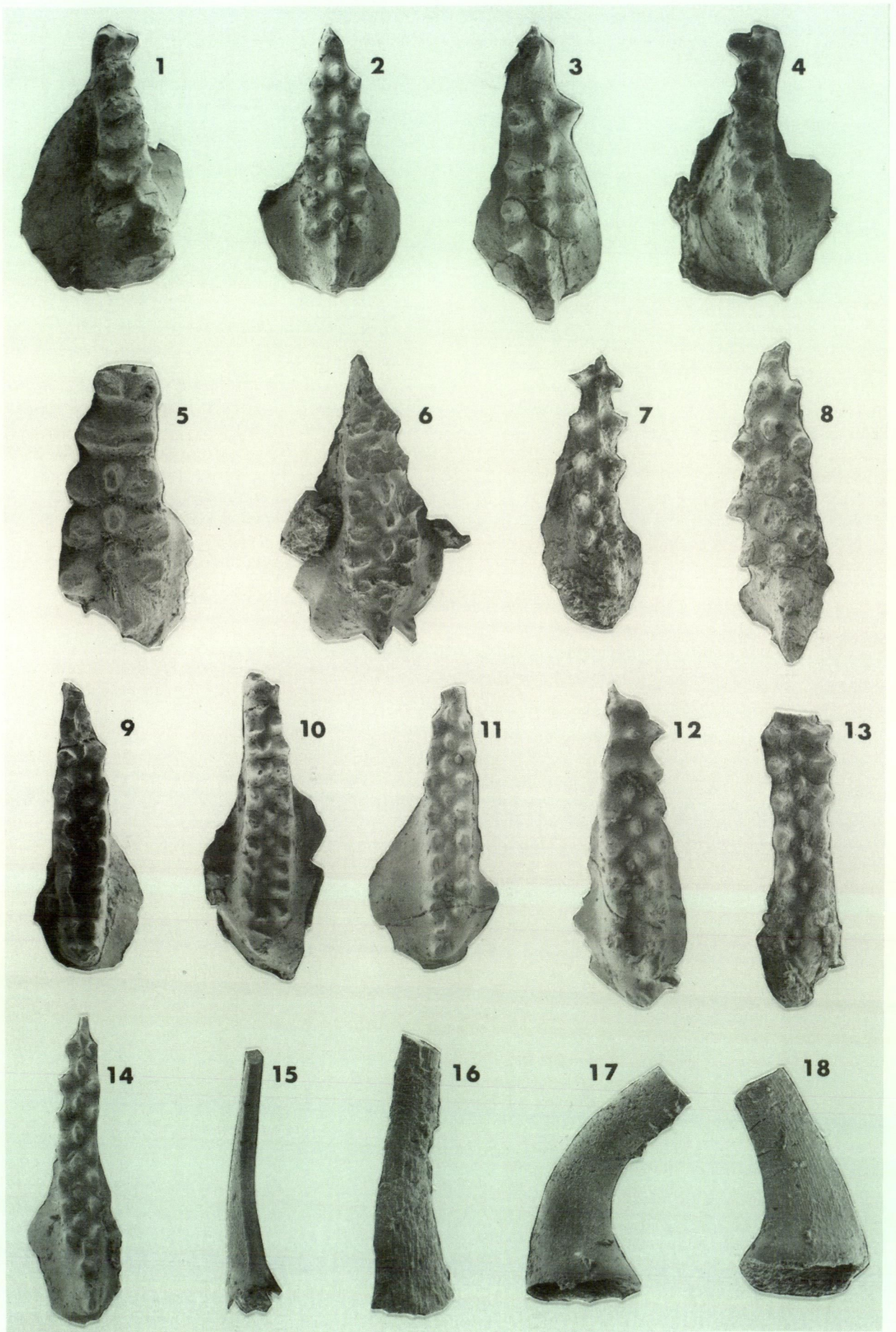
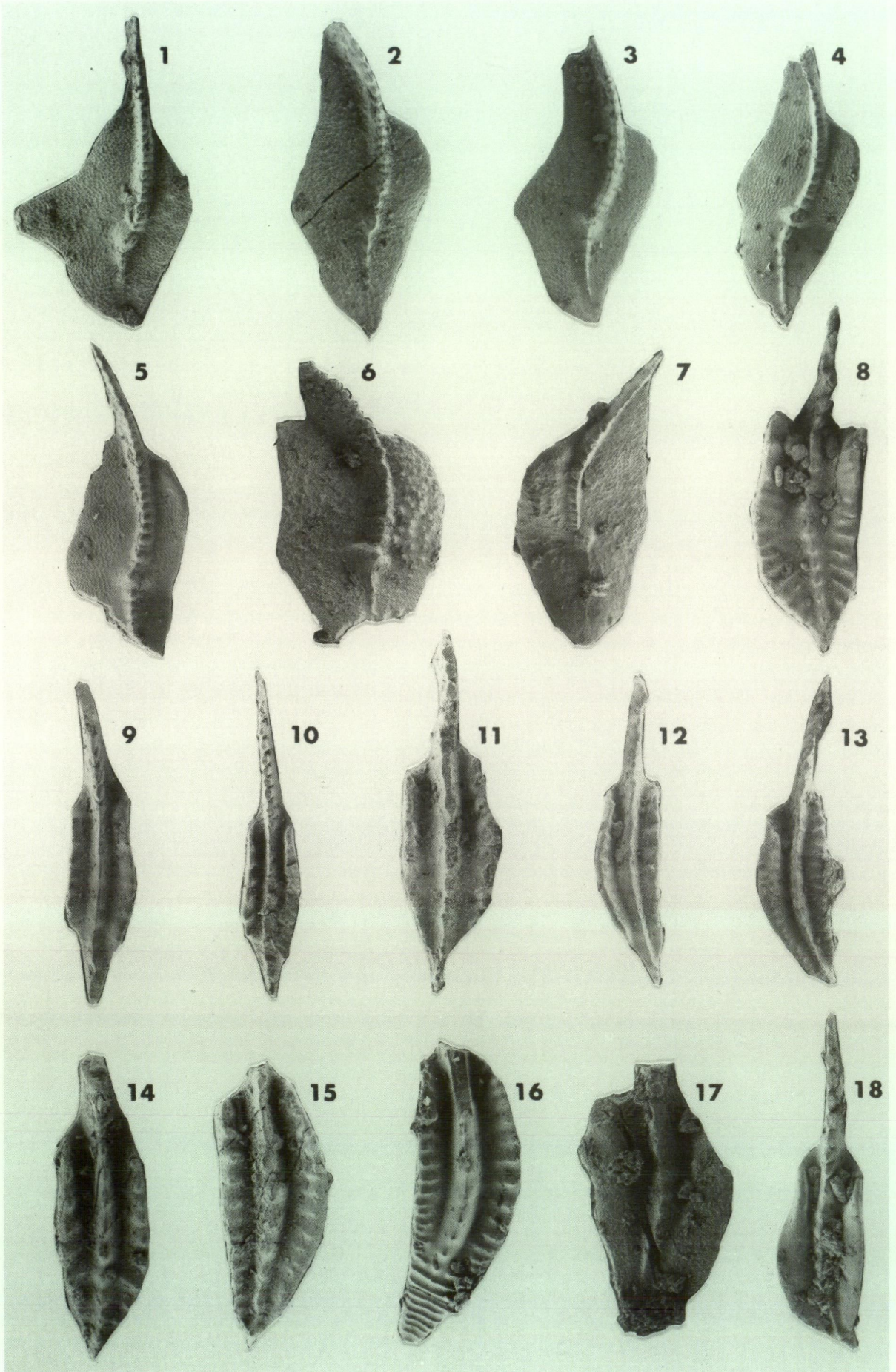


Figure 4 1, *Icriodus iowaensis iowaensis* Youngquist and Peterson. Upper view of I element, EUIC3033 from locality 1, x 80. 2–4, *Icriodus homeomorphus* Mawson. 2, upper view of I element, EUIC3033 from locality 1, x 130; 3, upper view of I element, EUIC30334 from locality 3, x 150; 4, upper view of I element, EUIC3035 from locality 1; x 85. 6–8, 14, *Icriodus alternatus alternatus* Branson and Mehl. 6, upper view of I element, EUIC3037 from locality 3, x 110; 7, upper view of I element, EUIC3038 from locality 2, x 170; 8, upper view of I element, EUIC3039 from locality 2, x 170; 14, upper view of I element, EUIC3045 from locality 4, x 110. 5, *Icriodus* cf. *alternatus alternatus*. Upper view of I element, EUIC3036 from Section A/23, x 170. 9–13, *Icriodus alternatus mawsonae* Yazdi. 9, upper view of I element, EUIC3040 from locality 1, x110; 10, upper view of I element, EUIC3041, x80; 11, upper view of I element, EUIC3042 from locality 1, x110; 12, upper view of I element, EUIC3043 from locality 1, x130; 13, upper view of I element, EUIC3044 from locality 2, x100. 15–18, *Pelekysgnathus inclinatus* Thomas. 15, lateral view of possible S element, EUIC3046 from locality 1, x 150; 16, lateral view of possible S element, EUIC3047 from Section B/8, x 150; 17, lateral view of possible S element, EUIC3048 from locality 1, x 220; 18, lateral view of possible S element, EUIC3049 from locality 1, x 200.



◀ **Figure 5** **1**, *Palmatolepis subperlobata* Branson and Mehl. Upper view of I element, EUIC3050 from locality 1, x 140. **2–4**, *Palmatolepis tenuipunctata* Sannemann. **2**, upper view of I element, EUIC3051 from locality 1, x 140; **3**, upper view of I element, EUIC3052 from locality 1, x 120; **4**, upper view of I element, EUIC3053 from locality 1, x 70. **5**, *Palmatolepis* sp. Upper view of broken I element, EUIC3054 from locality 1, x 120. **6, 7**, *Palmatolepis quadrantinosolobata* Sannemann. **6**, upper view of I element, EUIC3055 from locality 2, x 120; **7**, upper view of I element, EUIC30556 from locality 1, x 130. **8**, *Polygnathus pennatulus* Ulrich and Bassler. Upper view of Pa element, EUIC3057 from locality 1, x110. **9–11**, *Polygnathus brevilaminus* Branson and Mehl. **9**, upper view of Pa element, EUIC3058 from locality 1, x95; **10**, upper view of Pa element, EUIC3059 from locality 1, x95; **11**, upper view of Pa element, EUIC3060 from locality 1, x95. **12, 13**, *Polygnathus procerus* Sannemann. **12**, upper view of Pa element, EUIC3061 from locality 3, x120; **13**, upper view of Pa element, EUIC3062 from locality 1, x95. **16**, *Polygnathus semicostatus* Branson and Mehl. Upper view of broken Pa element, EUIC3065 from locality 3, x95. **14, 15**, *Polygnathus buzmakovi* Kuz'min. **14**, upper view of Pa element, EUIC3063 from locality 3, x130; **15**, upper view of broken Pa element, EUIC3064 from locality 3, x160. **17**, *Polygnathus communis communis* Branson and Mehl. Upper view of broken Pa element, EUIC3066 from Section A/13, x130. **18**, *Polygnathus* cf. *politus* Ovnatanova. Upper view of Pa element, EUIC3067 from Section A/6, x90.